



## Spin noise of conduction electrons in *n*-type bulk GaAs

Scott A. Crooker,<sup>1</sup> Lili Cheng,<sup>1</sup> and Darryl L. Smith<sup>2</sup>

<sup>1</sup>*National High Magnetic Field Laboratory, Los Alamos National Laboratory, Los Alamos, New Mexico 87545, USA*

<sup>2</sup>*Theoretical Division, Los Alamos National Laboratory, Los Alamos, New Mexico 87545, USA*

(Received 6 November 2008; published 29 January 2009)

We report a comprehensive study of stochastic electron spin fluctuations—spin noise—in lightly doped (*n*-type) bulk GaAs, which are measured using sensitive optical magnetometry based on off-resonant Faraday rotation. Frequency spectra of electron spin noise are studied as a function of electron density, magnetic field, temperature, probe-laser wavelength and intensity, and interaction volume. Electron spin lifetimes  $\tau_s$  are inferred from the width of the spin noise spectra and are compared to direct measurements of  $\tau_s$  using conventional Hanle-effect methods. Both methods reveal a strong and similar dependence of  $\tau_s$  on the wavelength and intensity of the probe laser, highlighting the undesired influence of sub-bandgap absorption effects on the nominally “nonperturbative” spin noise measurements. As a function of temperature, the spin noise power increases approximately linearly from 1.5 to 30 K, as expected for degenerate electrons obeying Fermi-Dirac statistics, but with an additional zero-temperature offset. Finally, as the cross-sectional area of the probe laser shrinks and fewer electrons are probed, the measured Faraday rotation fluctuations due to electron spin noise are shown to increase, as expected.

DOI: [10.1103/PhysRevB.79.035208](https://doi.org/10.1103/PhysRevB.79.035208)

PACS number(s): 72.25.Rb, 05.40.-a, 72.70.+m

### I. INTRODUCTION AND BACKGROUND

Not long after the discovery of nuclear magnetic resonance, Bloch<sup>1</sup> wrote in his seminal 1946 paper on *Nuclear Induction* that “even in the absence of any orientation by an external magnetic field one can expect in a sample with *N* nuclei of magnetic moment  $\mu$  to find a resultant moment of the order  $(N)^{1/2}\mu$  because of statistically incomplete cancellation.” Thirty-nine years later these small random fluctuations within a nuclear spin ensemble—spin noise—were directly observed by Sleator *et al.*<sup>2</sup> in a low-temperature nuclear quadrupole resonance study of <sup>35</sup>Cl nuclei in NaClO<sub>3</sub>. Subsequently, interest in spin noise phenomena has been growing steadily, particularly in recent years as experimental detection sensitivities continue to improve and as the characteristic sizes of probed spin ensembles grow ever smaller.<sup>3,4</sup> For example, proton nuclear spin noise was measured in liquid samples at room temperature<sup>5</sup> and a theory of nuclear spin noise and its detection was described.<sup>6</sup> More recently, spatial distributions of nuclear spin noise have been imaged,<sup>7,8</sup> an important step toward an alternative and “passive” approach to magnetic resonance imaging (MRI) that is based on a system’s intrinsic spin fluctuations alone.

In parallel with these efforts to detect nuclear spin noise, experiments to measure the stochastic fluctuations of *electronic* spins have been pursued, first by Aleksandrov and Zapassky<sup>9</sup> who used optical Faraday rotation to detect ground-state spin fluctuations in a gas of sodium atoms. Within the last decade, related techniques to detect electronic spin noise in atomic gases have been used to demonstrate spin squeezing and also to control quantum-mechanical entanglement.<sup>10–16</sup>

Recently, the frequency spectra of electron spin noise were explicitly studied in classical (warm) vapors of rubidium and potassium atoms.<sup>17,18</sup> In accord with the fluctuation-dissipation theorem, these noise signatures revealed the full magnetic resonance spectrum of the atomic

ground state without ever having to pump, excite, or otherwise perturb the spin ensemble away from thermal equilibrium. These experiments also used an off-resonant optical Faraday rotation probe to passively “listen” to the  $\sqrt{N}$  spin fluctuations of the ensemble. The probe laser in these studies was detuned by an energy  $\Delta$  from an atomic *S-P* optical resonance, ensuring no absorption of the laser (and therefore no perturbation of the atoms) to leading order. Nonetheless, random spin fluctuations in the atomic ground-state imparted Faraday rotation fluctuations on the laser via the dispersive (real) part of the vapor’s dielectric function—that is, through the spin-dependent indices of refraction<sup>19,20</sup> for circularly polarized light,  $n^\pm$ , which decay much more slowly with laser detuning ( $\sim\Delta^{-1}$ ) as compared to the absorption ( $\sim\Delta^{-2}$ ).

Similar optical approaches to measure electron spin noise in condensed-matter systems have now been demonstrated, notably in electron-doped (*n*-type) GaAs by Oestreich and co-workers.<sup>21,22</sup> These studies are especially noteworthy in view of the rapidly developing field of semiconductor spintronics<sup>23,24</sup> in that noise spectroscopy of electron spins can reveal important dynamic spin properties (such as spin-relaxation time and precession phenomena) *without* needing to inject additional electrons by optical or electrical means. In this context, perhaps the simplest and most well-studied system is the Fermi sea of spin-1/2 electrons that can form in the conduction band of doped direct-gap semiconductors such as GaAs. While much about this spin system is known from extensive pump-probe studies over the years, the spin noise properties of this “ideal” electron gas are only beginning to be explored.

To this end, this article reports on a comprehensive study of stochastic electron spin noise in lightly electron-doped (*n*-type) bulk GaAs, which we measure using a sensitive optical magnetometer based on sub-bandgap Faraday rotation. Frequency spectra of electron spin noise are measured as a function of electron density, applied transverse magnetic field, temperature, probe-laser wavelength and intensity, and

interaction volume. We infer electron spin lifetimes  $\tau_s$  from the width of the spin noise power spectra and compare these values with direct measurements of  $\tau_s$  obtained using conventional methods based on optical orientation of electron spins and the Hanle effect. Both methods reveal a strong dependence of  $\tau_s$  on the wavelength and intensity of the probe laser, highlighting the undesired influence of sub-bandgap absorption effects on these nominally “nonperturbative” spin noise measurements. With decreasing temperature from 30 to 1.5 K, the noise power from this sea of fluctuating electron spins decreases approximately linearly—as expected for degenerate electrons obeying Fermi-Dirac statistics—but with an interesting zero-temperature offset. Finally, we show that Faraday rotation fluctuations due to spin noise actually increase as the area of the probe-laser beam is reduced and fewer electrons are probed.

## II. EXPERIMENTAL DETAILS

Figure 1(a) shows a schematic of the optical magnetometer used to passively “listen” to electron spin noise in  $n$ :GaAs. It is very similar to that originally used to detect spin noise spectra in warm vapors of alkali atoms.<sup>17</sup> A probe-laser beam, derived from a continuous-wave Ti:sapphire ring laser, is tuned to the transparency region below the low-temperature band gap of bulk GaAs ( $E_{\text{gap}} \sim 1.515$  eV or  $\sim 818$  nm). This probe laser is linearly polarized and is focused through one of three silicon-doped ( $n$ -type) GaAs wafers that are mounted, strain free, in the variable-temperature insert of an optical <sup>4</sup>He cryostat. Typical probe-laser spot diameters range from 15–150  $\mu\text{m}$ .

The three bulk  $n$ :GaAs wafers (denoted A, B, and C) are antireflection coated and are 350, 170, and 170  $\mu\text{m}$  thick, with electron densities  $N_e = 1.4, 3.7, \text{ and } 7.1 \times 10^{16} \text{ cm}^{-3}$  at 10 K, respectively. These densities are near the critical density at which the metal-insulator transition occurs in  $n$ :GaAs ( $N_e^{\text{MIT}} \approx 2 \times 10^{16} \text{ cm}^{-3}$ ), where electron spin lifetimes  $\tau_s$  are known to be rather long at cryogenic temperatures, in the order of 100 ns.<sup>25–29</sup> A control wafer of semi-insulating GaAs was also studied and exhibited no detectable electron spin noise signal.

Random fluctuations of the electron spins along the  $\hat{z}$  direction,  $\delta S_z(t)$ , impart Faraday rotation fluctuations  $\delta\theta_F(t)$  on the transmitted probe-laser beam via the spin-dependent indices of refraction for right- and left-circularly polarized light  $n^\pm(\nu)$ , as discussed in more detail in Sec. III. These Faraday rotation fluctuations are detected and converted to a fluctuating voltage signal using a polarization beam splitter and a balanced photodiode bridge. We use either a 650 MHz bridge having 0.35 V/mW peak conversion gain (New Focus 1607) or a slower 80 MHz bridge having 20 V/mW peak conversion gain (New Focus 1807). The fluctuating voltage signals at the bridge output are amplified and then detected using fast digitizers, similar to the approach described recently by Römer *et al.*<sup>22</sup> Power spectra of these time-domain signals are computed with fast-Fourier-transform algorithms (using typical record lengths of  $2^{10}$  to  $2^{15}$  points) and are signal-averaged in software. Modest magnetic fields can be applied in the transverse direction ( $B \parallel \hat{x}$ ), which causes all

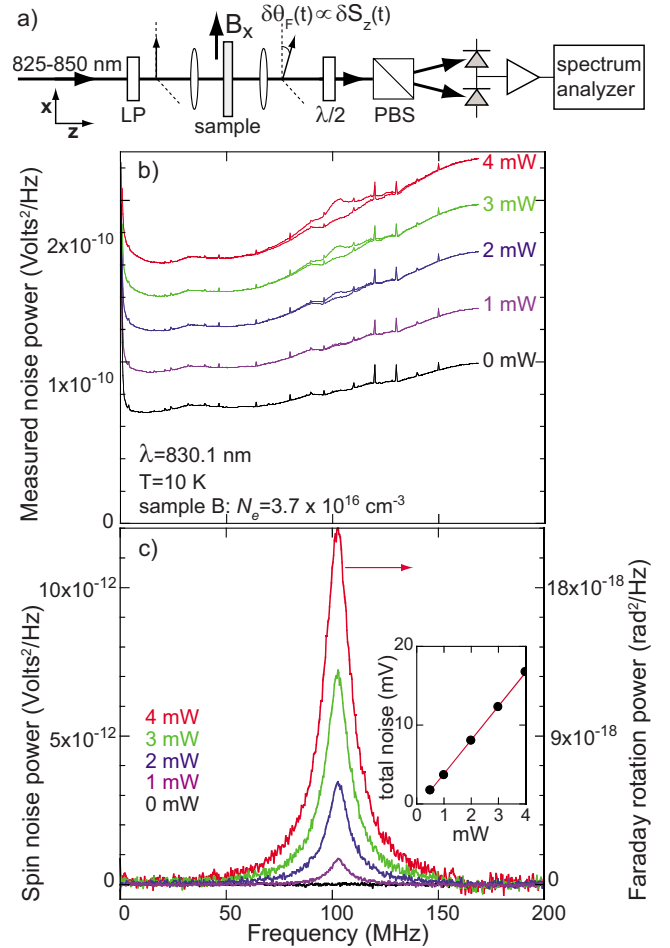


FIG. 1. (Color online) (a) The spin noise experiment, showing linear polarizer (LP), polarization beam splitter (PBS), and half-wave plate ( $\lambda/2$ ). (b) Raw spin noise data from an  $n$ :GaAs wafer (sample B) for transmitted probe-laser intensities from 0–4 mW. Data are not offset; the increasing noise power density arises from increasing photon shot noise. At each laser intensity, two spectra are acquired: one in the target transverse magnetic field (here,  $B_x = 175$  G) and one in a background field ( $B_x > 1000$  G). (c) Their difference reveals the extra noise power density due to fluctuating, precessing electron spins, shown in units of  $\text{V}^2/\text{Hz}$ . The 4 mW spectrum is also expressed as a Faraday rotation power density ( $\text{rad}^2/\text{Hz}$ ; right axis). Inset: The integrated spin noise in units of volts (or square-root of the integrated power) scales linearly with laser intensity. All these spectra have the same total integrated Faraday rotation noise:  $\sim 22.5 \mu\text{rad}$ .

spin fluctuations  $\delta S_z$  to precess about  $B_x$ . This shifts the peak of the spin noise away from zero frequency (where other environmental noise sources may exist) to the electron Larmor precession frequency  $\omega_L = g_e \mu_B B_x / \hbar$ , from which the electron  $g$  factor,  $g_e$ , can be measured ( $\mu_B$  is the Bohr magneton).

## III. SHORT THEORETICAL DESCRIPTION

Faraday rotation—the optical polarization rotation of linearly polarized light upon passage through a material—

results from unequal indices of refraction for right- and left-circularly polarized light,  $n^\pm(\nu)$ ,

$$\theta_F(\nu) = \frac{\pi\nu L}{c}[n^+(\nu) - n^-(\nu)], \quad (1)$$

where  $\nu$  is the frequency of the light,  $c$  is the speed of light, and  $L$  is the effective thickness of the material. In analogy with noise spectroscopy of alkali atoms,<sup>9,17</sup> a difference between refraction indices  $n^+(\nu)$  and  $n^-(\nu)$  arises near the band edge of GaAs when the net spin polarization of electrons in the conduction band is not zero. (The coupling between electron/hole spin orientation and circular optical polarization is given by the well-known optical selection rules in GaAs and related semiconductors,<sup>30</sup> which in turn derive from spin-orbit splitting in the valence band.)

In the absence of a magnetic field along the laser direction  $\hat{z}$ ,  $n^+ - n^-$  scales with the difference between spin-up and spin-down electron densities,  $N_e^+ - N_e^-$  (where the total electron density is  $N_e = N_e^+ + N_e^-$  and “spin-up” and “spin-down” denote electrons with spin projection antiparallel and parallel to  $\hat{z}$ ). For photon energies  $h\nu$  well below the GaAs band edge at  $h\nu_0$  (the latter being where absorption changes due to spin imbalances mainly occur), the energy dependence of the index difference  $n^+(\nu) - n^-(\nu)$  can be approximated using Kramers-Kronig relations to scale inversely with laser detuning,  $\Delta = \nu_0 - \nu$ . Thus for large detuning,

$$n^+(\nu) - n^-(\nu) \sim \frac{1}{\Delta}(N_e^+ - N_e^-). \quad (2)$$

Using Eq. (2) we can now capture generally how the magnitude of the detected spin noise depends on various external parameters. We will explicitly measure the dependence of  $n^+(\nu) - n^-(\nu)$  on detuning  $\Delta$ , using a fixed electron spin polarization, in Sec. IV D.

In these noise studies, the number of electrons  $N$  within a probe-laser beam of cross-sectional area  $A$  and over the sample thickness  $L$  is  $N = N_e AL$ . At zero magnetic field and in thermal equilibrium, this ensemble of  $N$  electrons has zero time-averaged spin polarization:  $\langle N^+ - N^- \rangle = 0$ . Electron spin noise, however, arises from statistical temporal fluctuations in the quantity  $N^+ - N^-$ , which have root-mean-square (rms) amplitude

$$\sqrt{\langle (N^+ - N^-)^2 \rangle} = \sqrt{fN} = \sqrt{fN_e AL}. \quad (3)$$

Here, the factor  $f$  accounts for the *fraction* of the electron spins that are allowed to fluctuate. For noninteracting electron spins such as those found in the warm (classical) alkali vapors studied previously<sup>17</sup> or, e.g., in the case of dilute paramagnetic impurities in a solid,<sup>3</sup> all  $N$  electrons fluctuate and  $f=1$ . In contrast, for degenerate electron systems obeying Fermi-Dirac statistics, only those electron spins within thermal energy  $\sim k_B T$  of the Fermi energy  $\epsilon_F$  have available phase space to fluctuate (all states at lower energy being occupied), in which case  $f < 1$ . For an ideal Fermi sea of electrons and in the absence of other correlations,<sup>31</sup>  $f \rightarrow 0$  as  $T \rightarrow 0$ . These considerations will be discussed in Sec. IV E, where the temperature dependence of the electron spin noise is measured. Our  $n$ :GaAs samples, being lightly doped near

the metal-insulator transition, are neither clearly in the low-doping limit (where electrons are localized on isolated donors and can be considered noninteracting) nor clearly in the high-doping limit (where  $\epsilon_F$  greatly exceeds the donor binding energy and Fermi-Dirac statistics of degenerate electrons dominate).

Combining Eqs. (1)–(3) and ignoring overall constants, the rms amplitude of Faraday rotation fluctuations due to electron spin noise in  $n$ :GaAs therefore scales as

$$\sqrt{\langle \theta_F^2 \rangle} \sim \frac{1}{\Delta} \sqrt{\frac{L}{A}} \sqrt{fN_e}. \quad (4)$$

This total spin noise—in units of radians of measured Faraday rotation—should therefore scale approximately inversely with laser detuning (measured explicitly in Sec. IV D) and inversely with the square root of the probe beam diameter (measured in Sec. IV F).

## IV. SPIN NOISE MEASUREMENTS

### A. Dependence on probe-laser intensity

An example of raw data from an electron spin noise experiment on  $n$ :GaAs is shown in Fig. 1(b). Here, the temperature of sample B is 10 K, the probe-laser wavelength is tuned below gap to 830.1 nm, and the intensity of the probe-laser beam at the output of the sample—that is, the transmitted laser intensity—is varied from 0 to 4 mW. (Note that in this paper we refer to the probe-laser power as an “intensity” so as to avoid potential confusion with the “noise power” that we measure). For each probe-laser intensity, noise power spectra at two transverse magnetic fields are acquired: one at the target field ( $B_x = 175$  G in this case) and one at a large background field (typically,  $B_x > 1000$  G) that shifts the spin noise out of the detected frequency range. The difference between these two power spectra [shown in Fig. 1(c)] reveals any extra noise power due to the probed ensemble of randomly fluctuating and precessing electron spins in the  $n$ :GaAs.

Unless otherwise stated, we measure and show spectra of the measured noise *power* density—that is, in units of (V)<sup>2</sup>/Hz of detected signal, or more usefully (since voltages vary trivially with detector and amplifier gains) in units of (rad)<sup>2</sup>/Hz of detected Faraday rotation. Frequency-integrated (or total) spin noise—see Eq. (4)—is computed from the measured noise power spectra and is expressed either as a total spin noise power ( $\langle \theta_F^2 \rangle$ , in units of rad<sup>2</sup>) or simply as a total spin noise ( $\sqrt{\langle \theta_F^2 \rangle}$ , in units of radians).

In Fig. 1(b), the noise power spectra at 0 mW—when the probe laser is turned off—reveals the background electronic noise floor of the amplified 650 MHz photodiode bridge output. Sharp features at specific frequencies are due to insufficiently shielded nearby radiofrequency sources. The increase of the background noise floor with increasing probe-laser intensity is due to additional “white” photon shot noise. Using  $\sim 3$  mW of transmitted probe laser, the photon shot noise power density is comparable to the electronic noise power density of these detectors. At about the same probe intensity, the extra noise due to fluctuating electron spins (at  $\sim 100$

MHz) becomes visible on this scale. Clearly, the spin noise signals from electrons in  $n$ :GaAs are smaller in terms of absolute noise power density than the background noise floor and signal averaging of several minutes to an hour is typically required.

The spin noise power spectra are much more clearly seen in the difference spectra of Fig. 1(c), for which the detector and photon shot noise contributions are subtracted away. The spin noise power spectra exhibit Lorentzian line shapes, indicating that the spin-spin correlation function,  $\langle S_z(t)S_z(0) \rangle$ , decays exponentially with characteristic spin-relaxation time  $\tau_s$ . The full width at half maximum of the spectral peaks,  $\Gamma$ , therefore reveals the inverse electron spin lifetime

$$\tau_s = 1/(\pi\Gamma). \quad (5)$$

The integrated area under these spectral peaks yields the total measured spin noise power, in units of  $V^2$  or  $\text{rad}^2$ . For a fixed peak width  $\Gamma$  and a fixed averaging time, the visibility of the spin noise peaks (or ratio of spin noise to background noise) improves with increasing probe-laser intensity. As shown in the inset of Fig. 1(c), doubling the probe intensity doubles the measured voltage fluctuations that are due to spin noise (and quadruples the measured power), while the background voltage density due to photon shot noise increases only by  $\sqrt{2}$ . Put another way, the integrated Faraday rotation induced by spin fluctuations is independent of probe-laser intensity [e.g.,  $\sqrt{\langle \theta_F^2 \rangle} \approx 22.5 \mu\text{rad}$  for all the noise spectra in Fig. 1(c)], but the Faraday rotation noise floor due to photon shot noise decreases as the inverse square root of the probe intensity.

### B. Dependence on transverse magnetic field, $B_x$

Figure 2(a) shows a series of electron spin noise power spectra from  $n$ :GaAs wafers A and C in the presence of applied transverse magnetic fields  $B_x$  from 0–300 G. The background noise floor from the detectors and from photon shot noise has been subtracted. The spin noise peaks shift to higher frequencies with increasing  $B_x$  as expected from the electron Larmor precession frequency,  $\omega_L = g_e \mu_B B_x / \hbar$ . However the two series of noise peaks do not shift at precisely the same rate. This can be more clearly seen in Fig. 2(b), which plots the spin noise frequency as a function of  $B_x$  for all three  $n$ :GaAs samples. The different slopes reveal the different low-temperature electron  $g$  factors in the three samples, which are found to decrease slightly in magnitude as the electron density (and therefore the Fermi energy  $\epsilon_F$ ) increases, in reasonable agreement with the established<sup>32</sup> energy dependence in GaAs,  $g_e(\epsilon_F) = -0.44 + 6.3 \text{ eV}^{-1} \times \epsilon_F$ .

Figure 2(a) also reveals that the widths  $\Gamma$  of the spin noise peaks from sample A are considerably narrower than those from sample C (4.5 MHz versus 16 MHz), implying a longer electron spin lifetime  $\tau_s$  ( $\sim 70$  ns versus  $\sim 20$  ns). While this relationship ultimately proves to be true for samples A and C, it should not strictly be inferred from the data shown in Fig. 2(a); Sec. IV C discusses how  $\tau_s$  can be adversely influenced (i.e., reduced) by external factors such as probe-laser wavelength, intensity, and spot size. Indeed, under very weak probe conditions sample A exhibits noise peaks narrower

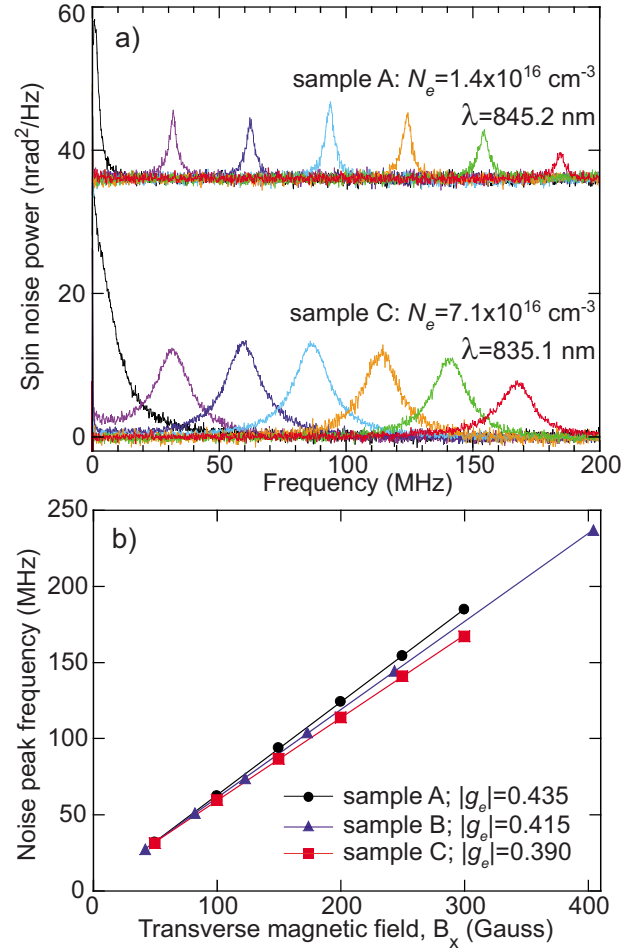


FIG. 2. (Color online) (a) Electron spin noise power spectra at 10 K from  $n$ :GaAs wafers A and C at  $B_x = 0, 50, 100, 150, 200, 250, 300$  G (black  $\rightarrow$  red). (b) The center frequency of these spin noise peaks versus  $B_x$  for all three  $n$ :GaAs wafers. The slope reveals the electron  $g$  factor,  $|g_e|$ .

than 1.8 MHz at 10 K, indicating that  $\tau_s > 175$  ns.

It is also apparent from these raw data that the area under the noise peaks varies slightly with  $B_x$ . However, these variations should not be considered significant here, as no attempt was made to correct for the frequency-dependent gain of the photodiodes, the amplifiers, or the digitizers (especially at high frequencies, where bandwidth-limiting filters attenuate incoming signals). Nor is it significant that in Fig. 2(a) the integrated spin noise power from sample C is larger than that from sample A. The experimental parameters were very different when these two samples were measured: not only were the probe-laser wavelengths different (845.2 nm for sample A versus 835.1 nm for sample C), but the sizes of the focused laser spots were different and the sample thicknesses themselves were different. As shown in Eq. (4), all these experimental parameters directly influence the total detected spin noise.

### C. Measuring electron spin lifetimes $\tau_s$ using spin noise spectroscopy

The intrinsic spin lifetimes  $\tau_s$  of conduction-band electrons in  $n$ :GaAs can, in principle, be inferred from the

widths  $\Gamma$  of spin noise power spectra [see Eq. (5)]. In the limit that the probe laser itself does not perturb the electronic states in the semiconductor (meaning, essentially, that no probe-laser photons are absorbed), then spin noise spectroscopy represents a passive and nonperturbative probe of time-dependent electron spin correlations. That is, spin dynamics are revealed through their stochastic fluctuations alone and no optical pumping or intentional optical orientation of electron spins is required, in contrast to most conventional pump-probe studies of electron spin dynamics which necessarily perturb the electron spin ensemble away from thermal equilibrium.<sup>25–29</sup> As suggested previously,<sup>17,21</sup> nonperturbative approaches based on spin noise may prove advantageous for studying the dynamics of electron spin systems at low temperatures, or (especially) for probing systems containing few spins, as demonstrated recently in the context of magnetic resonance force microscopy.<sup>3,4,33</sup>

In practice, however, we find that optical spin noise spectroscopy as applied to electrons in bulk  $n$ :GaAs can be significantly influenced by the undesired effects of probe-laser absorption even when probing well below the low-temperature band gap of GaAs. In contrast to optical spin noise spectroscopy of alkali vapors<sup>17</sup> (which have sharp atomic absorption resonances), it is considerably more challenging in bulk semiconductors to operate the probe laser in a regime that is clearly “nonperturbative,” while still retaining sufficient signal to measure. In large part this is due to the long low-energy exponentially decaying absorption tail (“Urbach tail”) that is characteristic of bulk semiconductors. As shown below, measurements of  $\tau_s$  via spin noise spectroscopy can be adversely influenced by the residual sub-bandgap absorption of the probe laser itself. Accurate measurements of  $\tau_s$  are shown to require either very little probe-laser intensity (in which case the spin noise signals are small, as shown in Fig. 1) or very large wavelength detunings below the GaAs band edge (in which case the noise signals are also very small, as per Eq. (4) and as also studied in Sec. IV D).

To illustrate these points, Figs. 3(a) and 3(b) show  $\tau_s$  measured in sample B at 10 K using spin noise spectroscopy. For reference, a schematic of the spin noise experiment is also shown. With the probe-laser wavelength at 830.1 nm, four noise power spectra are acquired using transmitted probe-laser intensities of 0.5, 1, 2, and 4 mW. The spin lifetime  $\tau_s$  inferred from the width  $\Gamma$  of these spectra are shown in Fig. 3(b). Clearly  $\tau_s$  is not constant, but rather decreases with increasing probe-laser intensity, indicating that absorption effects are adversely influencing the measurement.

To provide a direct comparison, we also measure  $\tau_s$  using “conventional” methods based on *intentional* optical orientation of electron spins and the Hanle effect. This experimental setup, sketched above Fig. 3(c), is identical to the setup for spin noise spectroscopy except that electron spins in the  $n$ :GaAs wafer are now partially aligned along  $\pm\hat{z}$  by an additional, above-band-gap (1.58 eV) defocused pump laser. The beam path and 25  $\mu\text{m}$  spot size of the probe laser on the sample is identical for the two methods. The polarization of the pump laser is modulated by a photoelastic modulator from left to right circular at 50 kHz, optically orienting electron spins parallel or antiparallel to  $\hat{z}$ . This small and con-

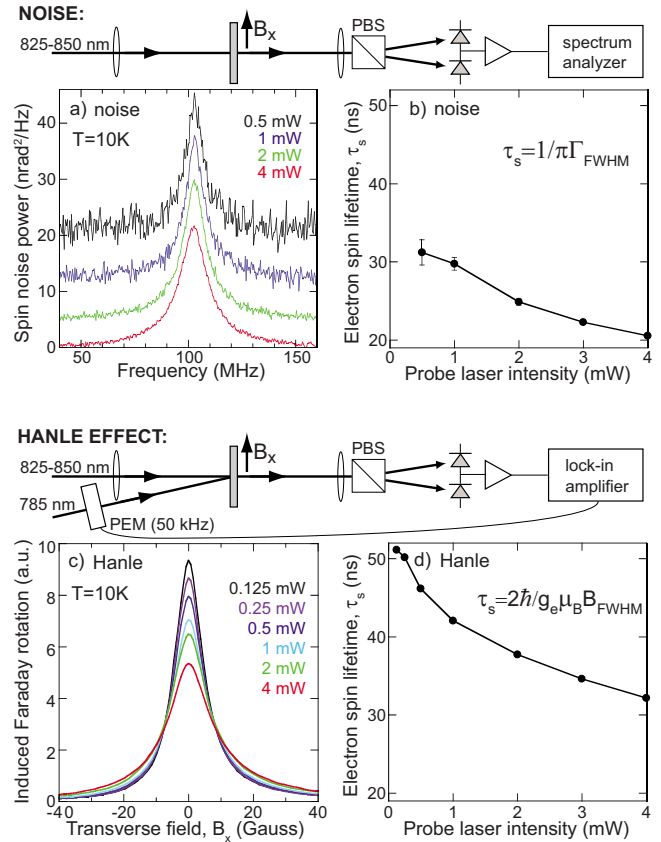


FIG. 3. (Color online) (a) The electron spin noise power in sample B at 10 K using transmitted probe-laser intensities of 0.5, 1, 2, and 4 mW ( $\lambda=830.1$  nm; spectra offset for clarity). (b) The spin lifetime  $\tau_s$  inferred from the width  $\Gamma$  of the noise spectra decreases with increasing probe-laser intensity. (c) Measuring  $\tau_s$  in sample B via optical spin orientation and “conventional” Hanle-effect methods using probe intensities from 0.125 to 4.0 mW. ( $\lambda=830.1$  nm) (d) The inferred  $\tau_s$  from these Hanle data also decreases with increasing probe-laser intensity.

stant electron spin polarization,  $S_z$ , imparts Faraday rotation  $\theta_F$  on the probe laser at this frequency, which is detected with lock-in amplifiers. Applied transverse magnetic fields  $B_x$  depolarize the injected spins by an amount that depends on  $\tau_s$ , leading to a reduction of the induced signal [see Fig. 3(c)]—this is the basis of the Hanle effect,<sup>30</sup> which is routinely used to measure  $\tau_s$  in GaAs and other semiconductors. These Hanle curves exhibit characteristic Lorentzian line shapes,  $\theta_F(B_x) \propto 1/[1+(g_e\mu_B B_x \tau_s/\hbar)^2]$ , with full widths  $B_{\text{fwhm}}=2\hbar/g_e\mu_B \tau_s$  from which the effective spin lifetime is revealed. We verify that we operate in the weak-pumping regime, where  $\theta_F$  scales linearly with (and  $\tau_s$  is independent of) pump-laser intensity. Figure 3(c) shows a series of Hanle curves from sample B at 10 K, where the probe-laser intensity is increased from 0.125 to 4 mW. The spin lifetimes extracted from these Hanle curves are shown in Fig. 3(d), where it is clear that—even though  $S_z$  is constant— $\tau_s$  decreases with increasing probe-laser intensity, similar to the trend exhibited by the spin noise measurements in Fig. 3(b).

To understand these results it is essential to independently measure the absorption and transmission characteristics of these  $n$ :GaAs wafers. Figure 4(a) shows the normalized

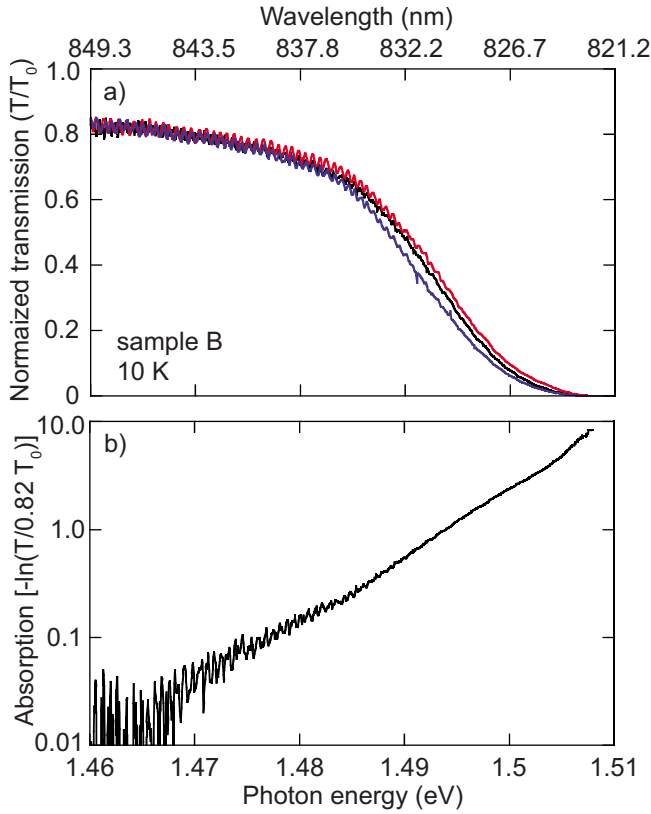


FIG. 4. (Color online) (a) The normalized optical transmission spectrum,  $T/T_0$ , through  $n$ :GaAs sample B at 10 K using different probe-laser intensities (the 10 K band gap of GaAs is  $\sim 1.515$  eV). (b) The same data plotted as an optical absorption (and assuming 18% reflection by the sample). The Urbach absorption tail persists well below the nominal GaAs band gap. Absorption at these subgap energies can reduce the electron spin lifetime that is measured by spin noise spectroscopy.

transmission of the probe laser through sample B at 10 K, for photon energies from 1.46 eV up to near the GaAs band gap at  $\sim 1.515$  eV. The blue, black, and red traces were acquired using transmitted probe-laser intensities of 0.04, 0.60, and 1.80 mW at 832 nm (1.49 eV). Differences between these traces arise from absorption and self-bleaching of the probe laser as it passes through the sample. The probe transmission is zero near the band edge (where absorption is strong) and increases to about 82% when the laser is tuned well below the band edge. The transmission does not saturate near 100% at low photon energies, likely due to some reflection of the probe laser by the  $\text{Si}_3\text{N}_4$  coating (similar behavior was observed from all of our coated  $n$ :GaAs wafers). Regardless, Fig. 4(a) indicates that sizeable absorption exists even at energies well below the GaAs band edge. To see this exponentially decaying absorption tail more clearly, Fig. 4(b) shows this data expressed as an optical-absorption constant ( $\alpha L$ ) and plotted on a semilog scale (and assuming 18% reflection).

Using these data it is possible to show that the changes in  $\tau_s$ , as measured either by spin noise spectroscopy or by conventional Hanle-effect methods, are directly correlated with the amount of probe-laser intensity that is *absorbed* by the  $n$ :GaAs wafer, independent of the actual probe-laser wave-

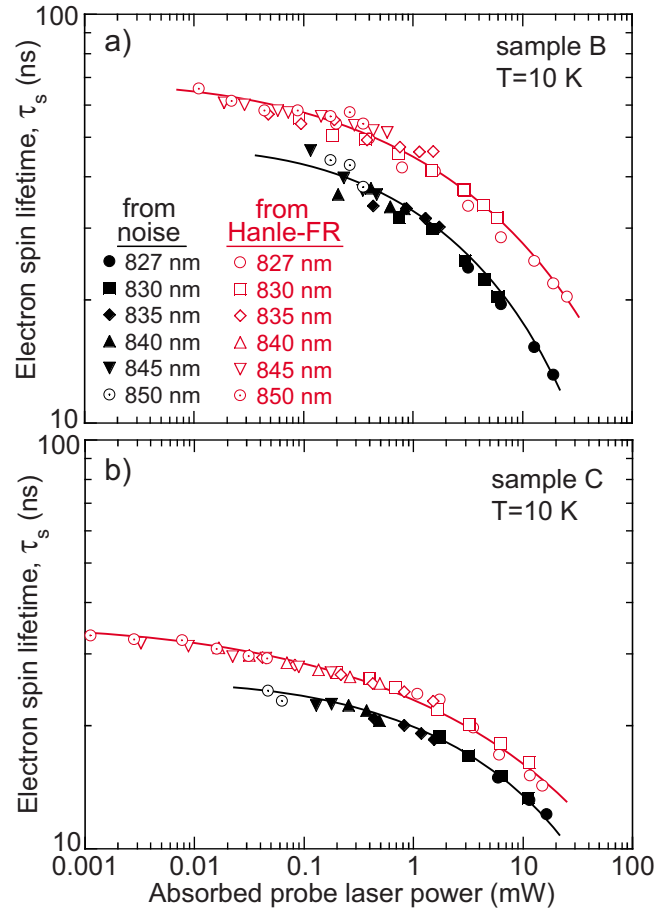


FIG. 5. (Color online) (a) A direct comparison of the electron spin lifetime  $\tau_s$  measured by spin noise methods (black points) and by conventional Hanle-effect methods (red points) in  $n$ :GaAs sample B at 10 K.  $\tau_s$  is shown on a log-log scale as a function of the probe-laser intensity that is *absorbed* by the sample. When plotted in this way, data from experiments using various probe-laser wavelengths and intensities collapse onto common curves (lines are guides to the eye). For both methods,  $\tau_s$  decreases significantly with absorbed probe-laser intensity, likely due to electron-hole creation by the probe-laser itself. (b) A similar comparison from  $n$ :GaAs sample C.

length or intensity. Figure 5 shows a compilation of data from samples B and C, where  $\tau_s$  was measured by both spin noise spectroscopy and also by the Hanle effect, using a variety of probe-laser wavelengths and intensities. When  $\tau_s$  is plotted as a function of the absorbed probe-laser intensity, all the points collapse onto a common curve. The strong reduction of  $\tau_s$  in the regime of large absorption very likely results from faster electron spin relaxation due to the density of photoexcited holes by the Bir-Aronov-Pikus (BAP) spin-relaxation mechanism.<sup>34</sup> The apparent spin lifetime increases by up to a factor of 3 in these studies as we approach the nonperturbative regime wherein few probe-laser photons are absorbed, either by tuning to very long wavelengths ( $\lambda > 845$  nm), by using very low probe-laser intensity, or both. Note that increasing the laser spot size has a similar effect (not shown), as this also reduces the photoexcited hole density. In the limit of small probe-laser absorption, the mea-

measured  $\tau_s$  approaches its intrinsic upper bound at 10 K ( $\sim 60$  ns for sample B and  $\sim 30$  ns for sample C), which is limited in these  $n$ -type samples by Dyakonov-Perel spin relaxation.<sup>30</sup>

While these two methods exhibit very similar trends as a function of absorbed probe intensity, they also reveal that  $\tau_s$  as measured by spin noise spectroscopy is consistently 30%–40% shorter than  $\tau_s$  measured by conventional Hanle methods. In principle, both methods should yield similar  $\tau_s$ . However, we note that noise-based spin lifetime studies of mobile spins are susceptible to transit-time effects, wherein the spins being measured diffuse out of the probed volume in a characteristic time that is shorter than the true spin-relaxation time. Transit-time broadening effects are well known in studies of atomic gases<sup>35</sup> (where spin lifetimes and therefore spin-diffusion lengths are very long) and may be important here in lightly doped bulk  $n$ :GaAs because the characteristic spin-diffusion length of electrons in these samples<sup>29</sup> is of order  $10 \mu\text{m}$ —comparable to the  $25 \mu\text{m}$  diameter of the focused laser spot. Noise measurements using larger spot diameters ( $>50 \mu\text{m}$ ) were found to yield longer  $\tau_s$  values, in better agreement with  $\tau_s$  measured by Hanle-effect methods.

Comparing the  $\tau_s$  measurements from spin noise spectroscopy and from the Hanle effect, it is clear that both methods are equally susceptible to the undesired effects of probe-laser absorption. Moreover, we find that—at least for bulk  $n$ :GaAs—a nonperturbative regime (in which the intrinsic  $\tau_s$  is accurately measured) is more easily achieved using conventional Hanle-effect methods. That is, both the pump and probe lasers can readily be made sufficiently weak so as not to adversely influence  $\tau_s$  and the measurements continue to exhibit very good signal-to-noise ratio within a few minutes' time [note the good signal-to-noise ratio of the data in Fig. 3(c) even when using very low probe-laser intensity]. In contrast, we find that spin noise spectroscopy using similar probe wavelengths and intensities requires considerably more signal averaging. We note that Hanle-effect methods based on photoluminescence<sup>26,27</sup> or magneto-optical Kerr effects<sup>28,29</sup> have been used in recent years to measure some of the longest spin lifetimes in  $n$ :GaAs—in excess of 500 ns in some cases.

#### D. Dependence on probe-laser detuning, $\Delta$

The magnitude of Faraday rotation fluctuations due to spin noise,  $\sqrt{\langle \theta_F^2 \rangle}$ , is expected to follow the energy dependence of the refraction index difference,  $n^+(\nu) - n^-(\nu)$ , as outlined earlier in Sec. III. In simple atomic systems having nearly ideal Lorentzian absorption resonances,  $n^+(\nu) - n^-(\nu)$  decays inversely with probe-laser detuning  $\Delta$  when the spin polarization is finite.<sup>17,20</sup> Faraday rotation fluctuations due to spin noise in alkali vapors were verified<sup>17</sup> to decrease as  $\Delta^{-1}$ , confirming that spin fluctuations coupled to the “passive” optical probe primarily through the dispersive indices of refraction and not through any absorptive effect.

To make a similar comparison in  $n$ :GaAs, where the band-edge absorption is considerably less idealized, the decay of  $n^+(\nu) - n^-(\nu)$  at energies below the band edge must be measured directly [the  $\Delta^{-1}$  scaling used in Eq. (2) was ap-

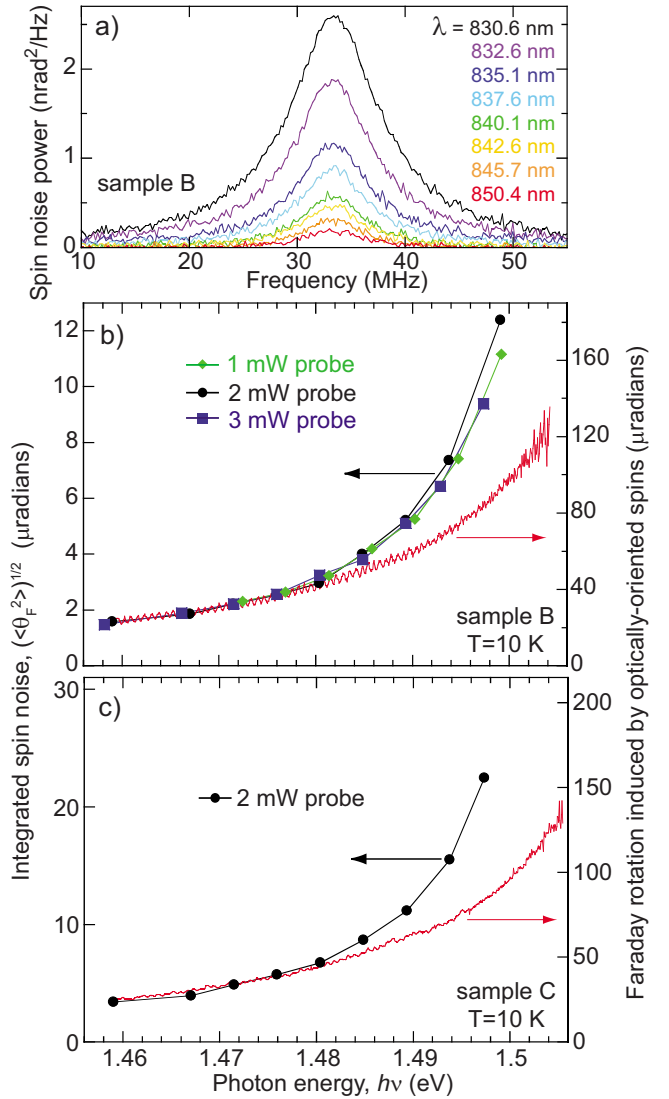


FIG. 6. (Color online) (a) Electron spin noise power spectra from  $n$ :GaAs sample B at 10 K, using sub-band-gap probe-laser wavelengths from 830.6 to 850.4 nm. For all spectra, the transmitted probe-laser intensity was 3 mW and  $B_x = 57$  G. (b) The integrated electron spin noise ( $\sqrt{\langle \theta_F^2 \rangle}$ , in microradians) versus probe-laser photon energy  $h\nu$ , for three probe-laser intensities. For comparison, the continuous red trace (right axis) shows  $\theta_F(\nu)$  induced by intentional optical orientation of electron spins in sample B using an additional 1.58 eV circularly polarized pump laser.  $\theta_F(\nu)$  decays as  $\sim \Delta^{-1}$ , assuming a GaAs band edge at 1.515 eV. (c) A similar comparison from sample C.

proximate for the purposes of outlining general trends]. Thus, here we aim to measure  $\sqrt{\langle \theta_F^2 \rangle}(\nu)$ , the energy dependence of Faraday rotation fluctuations due to spin noise in  $n$ :GaAs, and directly compare it to the independently measured decay of  $n^+(\nu) - n^-(\nu)$  in the presence of a small and fixed spin polarization.

Figure 6(a) shows a series of spin noise power spectra obtained from sample B at 10 K, where the probe-laser wavelength was tuned below the  $n$ :GaAs band edge from 830.6 to 850.4 nm (small  $\rightarrow$  large detuning). The transmitted probe-laser intensity was maintained at 3 mW and the probe

spot size and sample temperature were fixed. Clearly, electron spin noise induces larger Faraday rotation fluctuations as  $\Delta$  is reduced. The blue square points in Fig. 6(b) show the integrated spin noise  $\sqrt{\langle\theta_F^2\rangle}$  under these spectra (in microradians) as a function of probe-laser photon energy.

To interpret these data and to provide an accurate comparison, we independently measure  $n^+(\nu)-n^-(\nu)$  in sample B. This is accomplished by measuring the Faraday rotation  $\theta_F$  that is induced on the probe beam by a small and constant electron spin polarization  $S_z$  that is *intentionally* injected into the sample using an additional above-band-gap defocused and circularly polarized pump laser. This measurement uses the same experimental Hanle-effect setup described in Sec. IV C (and depicted in Fig. 3), but with  $B_x=0$  and with continuous tuning of the probe-laser wavelength. This small injected spin polarization perturbs the spin densities  $N_e^\pm$  in the  $n$ :GaAs wafer and therefore modifies the associated indices of refraction  $n^\pm(\nu)$  by a constant amount. The Faraday rotation of the transmitted probe laser therefore measures explicitly the photon energy dependence of  $n^+(\nu)-n^-(\nu)$ , which is shown by the continuous red curve in Fig. 6(b) (right axis). These studies were performed in the weak-pump and weak-probe limits, where  $\theta_F$  scaled linearly with pump intensity and was independent of probe intensity. Assuming a GaAs band gap at 1.515 eV and fitting the red curve to a power law,  $n^+(\nu)-n^-(\nu)$  does indeed decay very nearly as  $\Delta^{-1}$  (the fitted exponent is  $-1.06$ ).

Figure 6(b) therefore directly compares the energy dependencies of  $\sqrt{\langle\theta_F^2\rangle}$  (solid points) and  $n^+(\nu)-n^-(\nu)$  (red curve). The agreement between the two is reasonable at large detunings, i.e., at photon energies below  $\sim 1.48$  eV ( $\lambda > 838$  nm). For smaller detunings, the dependencies diverge—Faraday rotation fluctuations due to spin noise increase more rapidly than the Faraday rotation induced by a small fixed spin polarization.

While it is tempting to attribute this disparity to absorption effects and associated electron-gas heating (the measured spin noise *does* increase with temperature, as discussed in Sec. IV E), repeated studies using different probe-laser intensities do *not* exhibit any systematic changes. As shown in Fig. 6(b), nearly identical results were obtained using 1, 2, or 3 mW of transmitted probe laser (green, black, and blue points), suggesting that absorption effects are not adversely influencing the total spin noise. It may be that the different spin-polarization profiles of the two methods plays a role: whereas the fluctuating spin polarization that gives rise to spin noise exists throughout the entire wafer, the intentionally injected spin polarization  $S_z$  is generated only within a spin-diffusion length of the  $n$ :GaAs surface. However, possible surface effects have not been explicitly investigated in this work. Similar results were obtained in all the  $n$ :GaAs samples; Fig. 6(c) shows the results of a similar comparison in sample C.

### E. Dependence on temperature

The integrated spin noise that we measure in  $n$ :GaAs scales as the square root of the number of fluctuating electron spins. As discussed earlier [see Eqs. (3) and (4)], this number

may represent only a fraction  $f$  of the *total* number of electrons  $N$  if, being fermions, the electrons form a degenerate system and Fermi-Dirac statistics apply. In this case, only the electron spins within the thermal energy  $k_B T$  of the Fermi energy  $\epsilon_F$  have available phase space to fluctuate; all states at lower energies are fully occupied and spin fluctuations are suppressed. In an ideal electron gas, the number of fluctuating electrons  $fN$  can be estimated as

$$fN = V \int_0^\infty f(\epsilon)[1-f(\epsilon)]g(\epsilon)d\epsilon, \quad (6)$$

where  $V$  is the probed sample volume,  $f(\epsilon)$  is the Fermi-Dirac distribution using the appropriate (temperature-dependent) chemical potential, and  $g(\epsilon)$  is the density of states in the conduction band of bulk  $n$ :GaAs ( $\propto\sqrt{\epsilon}$ ). Therefore,  $fN$  is expected to be constant at high temperatures where the gas is classical and the electrons are noninteracting ( $k_B T \gg \epsilon_F$ ;  $f \sim 1$ ) and is expected to decrease when a degenerate electron gas forms upon cooling. At very low temperatures ( $k_B T < \epsilon_F$ ),  $fN$  is expected to decrease linearly to zero as  $T \rightarrow 0$ .

The measured temperature dependence of the spin noise power  $\langle\theta_F^2\rangle$ , which scales with  $fN$ , is shown in Fig. 7 for all three  $n$ :GaAs wafers, from  $T=30$  K down to  $T=1.5$  K. For all three samples, the measured noise power does indeed decrease approximately linearly as  $T \rightarrow 0$ , indicating that electrons in these  $n$ :GaAs samples do form degenerate electron systems to which Fermi-Dirac statistics apply. However, the most striking aspect of these data—observed in all three samples—is that  $\langle\theta_F^2\rangle$  does *not* appear to intercept the origin when the data are extrapolated to zero temperature. Rather, a finite amount of electron spin noise remains as  $T \rightarrow 0$ .

To ensure that inadvertent heating or absorption effects played no significant role, the temperature dependence of  $\langle\theta_F^2\rangle$  was measured multiple times on each sample using different probe-laser intensities, wavelengths, and spot sizes. To within overall scaling constants, the same temperature dependencies were observed, regardless of experimental conditions. The characteristic “noise” on these data may be inferred from the scatter of the data points and derives primarily from intensity drifts of the probe laser. In comparison with prior studies,<sup>22</sup> we do not observe any discontinuities or nonmonotonic behavior in the temperature dependence of  $\langle\theta_F^2\rangle$ .

This zero-temperature offset in the measured spin noise power is puzzling, but may derive from the fact that these  $n$ :GaAs wafers have electron densities  $N_e$  that are in the range of the critical metal-insulator transition density  $N_e^{\text{MIT}} \approx 2 \times 10^{16} \text{ cm}^{-3}$ . That is, these  $n$ :GaAs wafers are neither clearly in the high-doping regime (where the system is a good metal and Fermi-Dirac statistics overwhelmingly dominate) nor are they clearly in the low-doping regime (where electrons are localized and noninteracting). For very low electron densities  $N_e \ll N_e^{\text{MIT}}$ , where the system is best viewed as an ensemble of isolated and noninteracting electrons localized on their respective donors, Fermi-Dirac statistics are not expected to apply and all electrons are expected to fluctuate, giving a constant spin noise that is independent of



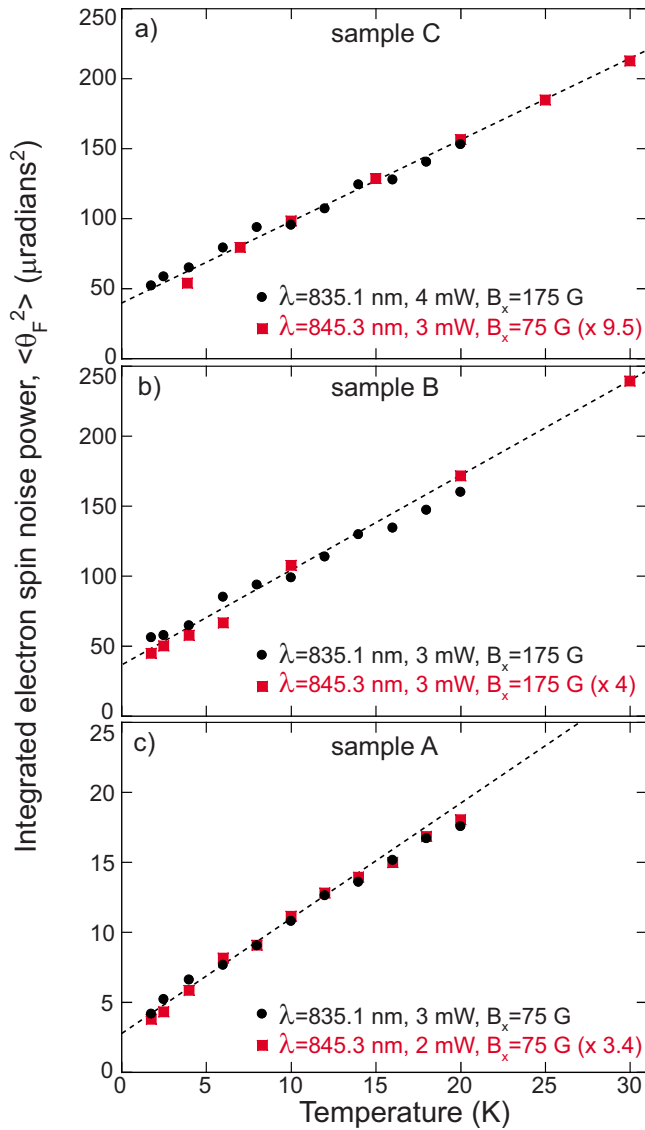


FIG. 7. (Color online) (a) The temperature dependence of the integrated electron spin noise power ( $\langle\theta_F^2\rangle$ , in units of  $\mu\text{radians}^2$ ) from  $n$ :GaAs sample C. Temperature sweeps corresponding to red and black points used different probe-laser wavelengths, intensities, and spot sizes, but are scaled so as to overlap. (b) and (c) Similar temperature dependencies from  $n$ :GaAs samples B and A. Dotted lines are linear guides to the eyes.

temperature. Very approximately, then, the trends observed in Fig. 7 may therefore result from the combined influence of electrons that are best described as mostly localized and electrons that are best described as mostly free. Measurements of spin noise in  $n$ :GaAs having significantly larger or smaller  $N_e$  should help elucidate these findings.

#### F. Dependence on probe-laser spot size

An often-mentioned advantage of noise-based spin measurements is the favorable scaling of spin noise signals with decreasing system size.<sup>3,7</sup> In an ensemble of  $N$  spins, the ratio of measured spin noise to the measured signal from a fully magnetized ensemble ( $\sim\sqrt{N}/N$ ) necessarily increases

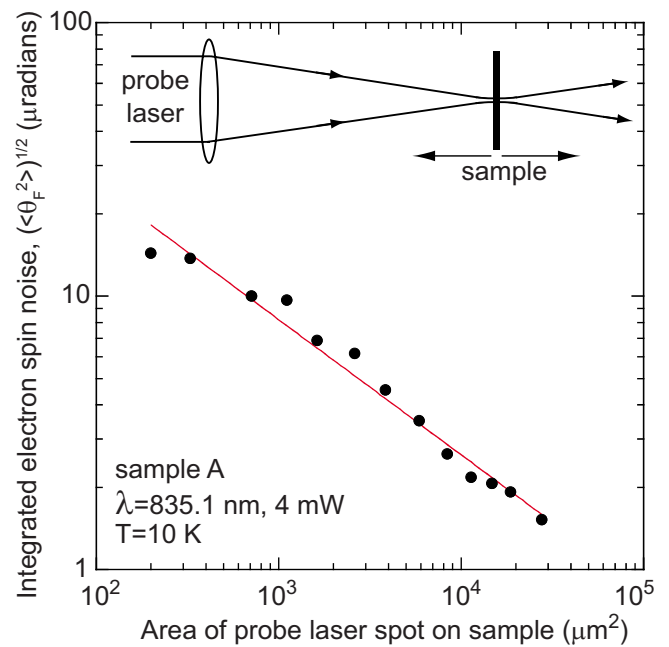


FIG. 8. (Color online) Log-log plot of the integrated Faraday rotation fluctuations due to electron spin noise ( $\sqrt{\langle\theta_F^2\rangle}$ , in units of microradians) in  $n$ :GaAs sample A as a function of the cross-sectional area of the probe-laser spot on the sample. The line shows a  $1/\sqrt{\text{area}}$  dependence, as expected for spin noise [see Eq. (4)]. Inset: The laser spot size was varied by translating the sample near the probe-laser focus and assuming Gaussian optics.

as  $N$  is reduced. In practice, it has been demonstrated that  $\sqrt{N}$  spin fluctuations can already exceed the thermal equilibrium (“Boltzmann”) magnetization of  $N$  paramagnetic spins in typical applied fields, when  $N$  (or equivalently, when the sample volume) is small.<sup>3,4</sup> Indeed, noise-based techniques were the basis for the recent detection of *single* electronic spins using ultrasensitive cantilevers<sup>33</sup> or scanning tunneling microscopes<sup>36–38</sup> and noise techniques will likely continue to provide the basis for detection of nuclear spin resonance in nanometer-scale structures.<sup>7,8</sup>

For fluctuating electron spins in  $n$ :GaAs, the advantageous scaling of noise signals with shrinking system size can be directly investigated by reducing the cross-sectional area of the probe-laser beam in the sample, as shown in Fig. 8. As the probe beam shrinks, the total integrated noise  $\sqrt{\langle\theta_F^2\rangle}$  increases as  $1/\sqrt{\text{area}}$ , in good agreement with Eq. (4). (Concurrently, the number of probed electrons  $N$  decreases from  $\sim 10^{11}$  to  $\sim 10^9$ ).

That not only the relative magnitude but the *absolute* magnitude of  $\sqrt{\langle\theta_F^2\rangle}$  increases with shrinking interaction volume is a consequence of the Faraday rotation detection method. An absolute increase in spin noise signal is not expected, for example, in conventional magnetometers that employ pickup coils. Consider a fully polarized spin ensemble: The Faraday rotation  $\theta_F$  imparted to a transmitted laser beam depends only on the areal density of spins  $N_e L$  and not on the total number of probed spins  $N$  [see Eq. (2)] and  $\theta_F$  is therefore independent of the beam’s cross-sectional area. Therefore, the effective sensitivity of the measurement—defined as the Faraday rotation per polarized spin,  $\theta_F/N$ —is larger in

smaller beams that probe fewer spins. Spin fluctuations, which scale as  $\sqrt{N}$ , therefore induce correspondingly more Faraday rotation when using smaller beams.

## V. SUMMARY

In bulk  $n$ :GaAs, spin noise spectroscopy using sub-bandgap Faraday rotation revealed the dynamical properties of conduction-electron spins ( $\tau_s, g_e$ ) through their fluctuation spectra alone in keeping with the fluctuation-dissipation theorem. Spin noise spectra were studied as a function of electron concentration, magnetic field, temperature, probe-laser wavelength and intensity, and sample volume. On the balance, these measurements indicated that the integrated area, frequency, and width of these spin noise spectra were in reasonable agreement with a simple model [Eq. (4)].

However, systematic studies also made clear that this optical approach to spin noise spectroscopy—at least as applied to bulk  $n$ :GaAs—is by no means a panacea. These noise methods are susceptible to undesired absorption of the probe laser, even in the nominal transparency region below the GaAs band edge (Figs. 3–5). Absorption effects ultimately lead to incorrect values of the intrinsic electron spin lifetime  $\tau_s$ , unless care is taken to operate the probe laser in a regime that is demonstrably nonperturbative (long wavelengths  $\lambda > 845$  nm, low intensities, and/or large spot sizes), in which case the spin noise signals are very small. We found, moreover, that accurate measurements of  $\tau_s$  are more readily and quickly obtained using conventional techniques based on the Hanle effect and intentional optical orientation. Nonetheless we posit that these limitations may be somewhat relaxed in

cleaner or lower-dimensional semiconductor structures that have less-pronounced absorption tails.

Some puzzles remain. The zero-temperature offset observed in the temperature dependence of the spin noise (Fig. 7) is against simple expectations of an ideal Fermi gas, but may arise in these bulk  $n$ :GaAs samples from the localizing influence of the embedded silicon donors. Also, the divergence between the energy dependencies of the spin noise and the refraction index difference at small laser detuning (Fig. 6) is not understood at this time.

Nonetheless, the outlook for optical spectroscopy of electron spin noise in semiconductors is promising. Clear signatures of conduction-electron spin noise are measurable in  $n$ :GaAs under a variety of conditions and they reveal important dynamical information about the spins themselves. The favorable scaling of spin noise signals with reduced system size (Fig. 8) suggests its use for studying spin correlations in mesoscopic electron ensembles, as very recently reported.<sup>39</sup> Finally, recent proposals for spin noise spectroscopy using time-delayed pairs of ultrafast laser pulses can potentially extend measurable noise bandwidths out to terahertz frequencies,<sup>40</sup> while application of oscillating magnetic fields may permit the observation of multiphoton phenomena in the spin noise.<sup>41</sup>

## ACKNOWLEDGMENTS

We thank Shanalyn Kemme at Sandia National Laboratory for antireflection-coating the GaAs wafers and we are indebted to Bogdan Mihaila, Peter Littlewood, and Sasha Balatsky for valuable discussions. We acknowledge support from the Los Alamos LDRD program and the National High Magnetic Field Laboratory.

- 
- <sup>1</sup>F. Bloch, *Phys. Rev.* **70**, 460 (1946).  
<sup>2</sup>T. Sleator, E. L. Hahn, C. Hilbert, and J. Clarke, *Phys. Rev. Lett.* **55**, 1742 (1985).  
<sup>3</sup>H. J. Mamin, R. Budakian, B. W. Chui, and D. Rugar, *Phys. Rev. Lett.* **91**, 207604 (2003).  
<sup>4</sup>H. J. Mamin, R. Budakian, B. W. Chui, and D. Rugar, *Phys. Rev. B* **72**, 024413 (2005); C. L. Degen, M. Poggio, H. J. Mamin, and D. Rugar, *Phys. Rev. Lett.* **99**, 250601 (2007).  
<sup>5</sup>M. Guéron and J. L. Leroy, *J. Magn. Reson.* (1969-1992) **85**, 209 (1989); M. A. McCoy and R. R. Ernst, *Chem. Phys. Lett.* **159**, 587 (1989).  
<sup>6</sup>D. I. Hoult and N. S. Ginsberg, *J. Magn. Reson.* **148**, 182 (2001).  
<sup>7</sup>N. Müller and A. Jerschow, *Proc. Natl. Acad. Sci. U.S.A.* **103**, 6790 (2006).  
<sup>8</sup>H. J. Mamin, M. Poggio, C. L. Degen, and D. Rugar, *Nat. Nanotechnol.* **2**, 301 (2007).  
<sup>9</sup>E. B. Aleksandrov and V. S. Zapassky, *Zh. Eksp. Teor. Fiz.* **81**, 132 (1981); *Sov. Phys. JETP* **54**, 64 (1981).  
<sup>10</sup>J. L. Sørensen, J. Hald, and E. S. Polzik, *Phys. Rev. Lett.* **80**, 3487 (1998).  
<sup>11</sup>A. Kuzmich, L. Mandel, J. Janis, Y. E. Young, R. Ejnisman, and N. P. Bigelow, *Phys. Rev. A* **60**, 2346 (1999); A. Kuzmich, L. Mandel, and N. P. Bigelow, *Phys. Rev. Lett.* **85**, 1594 (2000).  
<sup>12</sup>B. Julsgaard, A. Kozhekin, and E. S. Polzik, *Nature* (London) **413**, 400 (2001).  
<sup>13</sup>J. M. Geremia, J. K. Stockton, and H. Mabuchi, *Science* **304**, 270 (2004).  
<sup>14</sup>T. Yabuzaki, T. Mitsui, and U. Tanaka, *Phys. Rev. Lett.* **67**, 2453 (1991).  
<sup>15</sup>T. Mitsui, *Phys. Rev. Lett.* **84**, 5292 (2000).  
<sup>16</sup>M. Martinelli, P. Valente, H. Failache, D. Felinto, L. S. Cruz, P. Nussenzweig, and A. Lezama, *Phys. Rev. A* **69**, 043809 (2004).  
<sup>17</sup>S. A. Crooker, D. G. Rickel, A. V. Balatsky, and D. L. Smith, *Nature* (London) **431**, 49 (2004).  
<sup>18</sup>B. Mihaila, S. A. Crooker, D. G. Rickel, K. B. Blagoev, P. B. Littlewood, and D. L. Smith, *Phys. Rev. A* **74**, 043819 (2006).  
<sup>19</sup>Spin-orbit coupling in the excited  $P$  levels of alkali atoms mandate that spin-up and spin-down electrons in the atomic ground-state couple selectively to right- and left-circularly polarized light, analogous to the optical selection rules near the band edge of GaAs.  
<sup>20</sup>W. Happer and B. S. Mathur, *Phys. Rev. Lett.* **18**, 577 (1967).  
<sup>21</sup>M. Oestreich, M. Römer, R. J. Haug, and D. Hägele, *Phys. Rev. Lett.* **95**, 216603 (2005).  
<sup>22</sup>M. Römer, J. Hübner, and M. Oestreich, *Rev. Sci. Instrum.* **78**,

- 103903 (2007).
- <sup>23</sup> *Semiconductor Spintronics and Quantum Computation*, edited by D. D. Awschalom, D. Loss, and N. Samarth (Springer, Berlin, 2002).
- <sup>24</sup> I. Žutić, J. Fabian, and S. Das Sarma, *Rev. Mod. Phys.* **76**, 323 (2004).
- <sup>25</sup> J. M. Kikkawa and D. D. Awschalom, *Phys. Rev. Lett.* **80**, 4313 (1998).
- <sup>26</sup> R. I. Dzhioev, K. V. Kavokin, V. L. Korenev, M. V. Lazarev, B. Y. Meltser, M. N. Stepanova, B. P. Zakharchenya, D. Gammon, and D. S. Katzer, *Phys. Rev. B* **66**, 245204 (2002).
- <sup>27</sup> R. I. Dzhioev, V. L. Korenev, I. A. Merkulov, B. P. Zakharchenya, and D. Gammon, Al. L. Efros, and D. S. Katzer, *Phys. Rev. Lett.* **88**, 256801 (2002).
- <sup>28</sup> M. Furis, D. L. Smith, S. A. Crooker, and J. L. Reno, *Appl. Phys. Lett.* **89**, 102102 (2006).
- <sup>29</sup> M. Furis, D. L. Smith, S. Kos, E. S. Garlid, K. S. M. Reddy, C. J. Palmstrøm, P. A. Crowell, and S. A. Crooker, *N. J. Phys.* **9**, 347 (2007).
- <sup>30</sup> M. I. Dyakonov and V. I. Perel, in *Optical Orientation*, edited by F. Meier and B. Zakharchenya (North-Holland, Amsterdam, 1984), pp. 11–71.
- <sup>31</sup> B. Mihaila, S. A. Crooker, K. B. Blagoev, D. G. Rickel, P. B. Littlewood, and D. L. Smith, *Phys. Rev. A* **74**, 063608 (2006).
- <sup>32</sup> M. A. Hopkins, R. J. Nicholas, P. Pfeffer, W. Zawadzki, D. Gauthier, J. C. Portal, and M. A. DiForte-Poisson, *Semicond. Sci. Technol.* **2**, 568 (1987).
- <sup>33</sup> D. Rugar, R. Budakian, H. J. Mamin, and B. W. Chui, *Nature (London)* **430**, 329 (2004).
- <sup>34</sup> G. L. Bir, A. G. Aronov, and G. E. Pikus, *Zh. Eksp. Teor. Fiz.* **69**, 1382 (1975).
- <sup>35</sup> G. E. Katsoprinakis, A. T. Dellis, and I. K. Kominiis, *Phys. Rev. A* **75**, 042502 (2007).
- <sup>36</sup> C. Durkan, *Contemp. Phys.* **45**, 1 (2004).
- <sup>37</sup> P. Messina, M. Mannini, A. Caneschi, D. Gatteschi, L. Sorace, P. Sigalotti, C. Sandrin, S. Prato, P. Pittana, and Y. Manassen, *J. Appl. Phys.* **101**, 053916 (2007).
- <sup>38</sup> Z. Nussinov, M. F. Crommie, and A. V. Balatsky, *Phys. Rev. B* **68**, 085402 (2003).
- <sup>39</sup> G. M. Müller, M. Römer, D. Schuh, W. Wegscheider, J. Hübner, and M. Oestreich, *Phys. Rev. Lett.* **101**, 206601 (2008).
- <sup>40</sup> S. Starosielec and D. Hägele, *Appl. Phys. Lett.* **93**, 051116 (2008).
- <sup>41</sup> M. Braun and J. König, *Phys. Rev. B* **75**, 085310 (2007).